

Experimental and numerical study of nonlinear dynamic behaviour of an aerofoil

S. Fichera¹, S. Jiffri¹, X. Wei¹, A. Da Ronch², N. Tantaroudas¹ and J. E. Mottershead¹

¹ University of Liverpool,
Liverpool, L69 3GH, United Kingdom

² University of Southampton,
Southampton, SO17 1BJ, United Kingdom

Abstract

The paper describes the experimental and numerical investigations on a plunge-pitch aeroelastic system with a hardening nonlinearity. The goals of this work are to achieve a better understanding of the behaviour of the model while it undergoes Limit Cycle Oscillations and to tune the numerical model to reproduce both linear and nonlinear aeroelastic response observed in the aeroelastic system. Moreover, this work is part of an overall project, which final aims are to test various control strategies for flutter suppression on the nonlinear aeroelastic system. The experimental model consists of a rigid wing supported by adjustable vertical and torsional leaf springs provided with a trailing edge control surface. In the present work the rig is extended to include a nonlinearity introduced by connecting the plunge degree of freedom to a perpendicular pre-tensioned cable. The numerical model is a 2 *dof* reduced order model representing the dynamics properties of the real system, the nonlinearity is incorporated in the state space equations by adding the cubic and fifth order terms in the stiffness matrix; the unsteady aerodynamic is modelled with strip theory and the incompressible two-dimensional classical theory of Theodorsen. In addition to provide a comparison with the experimental results, the numerical model has been used during the course of the project as an interactive tool to guide the choice of the stiffness setting of the system. A comparison between experimental and numerical results is provided as well; for the linear model, they show a good agreement in the linear case, albeit not so much with the damping ratios. Once the nonlinearity is added, good agreement is achieved with the plunge LCO, but there still is room for improvement with pitch LCO. An in-depth investigation will be carried out to improve model tuning with respect to all parameters of the model.

1 Introduction

The research on nonlinear aeroelasticity has been a subject of high interest for the last two decades due to many events (Croft [4]) that occurred as a consequence of it. The well known aero-servo-elastic aspects are coupled with structural and/or aerodynamic nonlinearity giving rise to a nonlinear aeroelastic behaviour and, usually, its related Limit Cycle Oscillations (LCO).

The LCO [6] is a non-diverging, self-sustained, fixed-frequency structural oscillation. It can have a major deteriorating effects on the handling qualities of the aircraft, can cause fatigue in the long term and can prevent the release of armaments from the aircraft due to high amplitude oscillations. The result of LCO often places a restriction on the airplane flight envelope. Yet sometimes, this oscillation is welcome because, without it, the LCO would instead be replaced by catastrophic flutter leading to the loss of the flight vehicle.

Woolston *et al.* [12] investigated nonlinearities in structural stiffness and control surfaces linkages. They

created several models with freeplay, hysteresis, cubic-hardening and cubic-softening nonlinearities in the torsion mode. For general wing motion, they observed that the flutter velocity decreased as the initial disturbance increased, and that the stability of the system was highly dependent on the initial condition. A cubic-softening spring stiffness lowered the flutter velocity. They also noted that cubic hardening caused limit cycle oscillations rather than flutter at velocities above the open-loop flutter velocity.

Todd *et al.* [8] designed and studied the aeroelastic response of a rigid wing supported by nonlinear springs (NATA). Their analytical results are in good agreement with that of Woolston *et al.* [12] and the results from experimental studies utilizing the test apparatus.

For these reasons, at the University of Liverpool (UoL) during the last few years, has been developed and validated (see Papatheou *et al.* [10, 9]) firstly an experimental model of a linear two degrees of freedom (*dof*) aerofoil, schematically shown in Figure 1, to which has been added recently a hardening nonlinearity at the plunge *dof*.

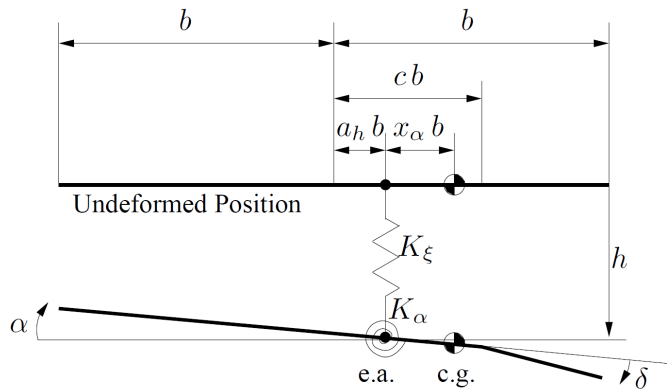


Figure 1: Schematic of a two-degree of freedom aeroelastic system.

The goals of this work are:

- to achieve a better understanding of the behaviour of the described configuration,
- to verify and tune the numerical model in order to have a suitable environment for the development of different LCO control algorithms.

This paper will present firstly the description of the linear experimental rig and the approach used to introduce the nonlinearity in an experiment. Then the numerical model will be depicted and a comparison between the numerical and the experimental results will be shown.

2 Description of the Experimental Rig

The wind tunnel experimental rig consists of a rigid wing section of a NACA 0018 aerofoil, with a chord (c) of 0.35 m and a span (b) of 1.2 m, supported by adjustable vertical and torsional leaf springs from each side, as shown in Figure 2. A high-stiffness torque tube connect externally the tips of the wing ensuring the absence of wing twist. The total mass of the model, including the external structure, is 6.5 kg. The aerofoil is provided with a single trailing edge central control surface (chord = 25% c , span = 35% b), see Figure 2b, driven by a V-stack piezoelectric actuator [1], that allows a maximum deflection of $\pm 7^\circ$ with a bandwidth of 15 Hz.¹ Preliminary tests were made to guarantee that the flexible modes of the wing, i.e. spanwise bending and torsion modes, are well above the pitch and plunge frequencies, and a separation of over one order of

¹When not used, the control surface is restrained by a tape to the rest of the wing.

magnitude was found. More details on the (linear) baseline aeroelastic wind tunnel model were presented in Ref. [9].

The model was tested in the University of Liverpool low-speed, open-loop wind tunnel; this facility has a maximum operating speed of 18 m/s and a test section of $1.2 \text{ m} \times 0.4 \text{ m} \times 1.0 \text{ m}$. Two laser sensors were mounted externally to the working section to measure the displacements of two points attached to the aerofoil shaft. The pitch and plunge degrees of freedom are readily available from these measurements.

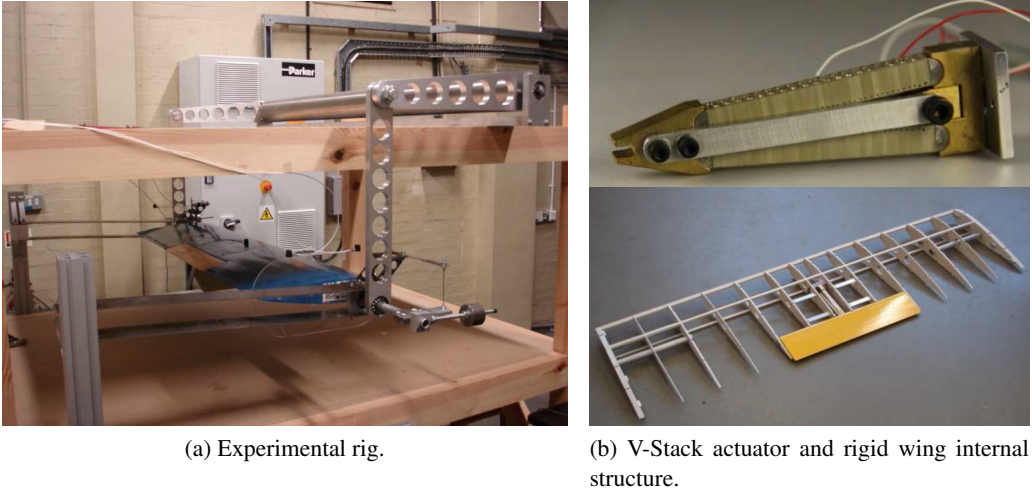


Figure 2: Schematic view of the experimental setup of the aeroelastic model in the University of Liverpool.

2.1 Description of the nonlinearity

The experimental rig just introduced was modified to introduce a concentrated hardening nonlinearity in the plunge degree of freedom [2]. The nonlinearity in the restoring force on each tip of the wing is realised by a clamped cable under tension, which acts as a hardening spring. Figure 3 shows the system of cables used to introduce the nonlinearity in the wind tunnel rig.

As known, the linear coefficient of the wire nonlinear restoring force is dependent only from the amount of pretension, while the cubic and the fifth order terms are dominated by the length of the wire, its elastic modulus and cross section.

Figure 4b shows the measured points for the nonlinear case along with a polynomial fit. The nonlinear relation between vertical force and plunge displacement is formulated as shown in eq. (1) where the constants, Table 4a, were calculated by a least-squares fit on experimental data.

$$F_{nl} = (K_{\xi 1} + K_{\xi})h + K_{\xi 3}h^3 + K_{\xi 5}h^5 \quad (1)$$

3 Description of the numerical model

A numerical aeroelastic model has been used alongside the wind tunnel experiments in this work. The model has served the following purposes:

- Guiding the choice of pitch and plunge stiffness values in the aerofoil rig that ensure sufficient separation between pitch and plunge modes, and also give rise to a flutter speed that is adequately below the maximum achievable airspeed in the wind tunnel.

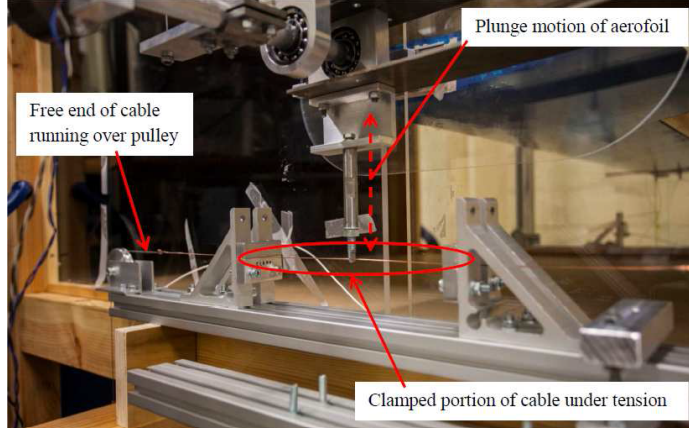


Figure 3: Schematic view of the system of cables used to introduce a nonlinearity in the wind tunnel test rig.

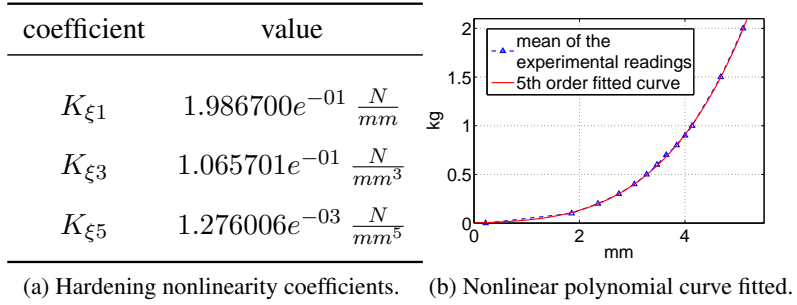


Figure 4: Hardening nonlinearity.

- Guiding the choice of parameters describing the hardening nonlinearity.
- Simulating time-domain nonlinear response and comparing LCO frequency and amplitude.

A brief description of the model is now presented.

3.1 Unsteady pitch-plunge aeroelastic model

The numerical model used by Da Ronch *et al.* [5] is employed in the present work. The linear, non-dimensional model is expressed by

$$\begin{bmatrix} 1 & \frac{x_\alpha}{r_\alpha^2} \\ x_\alpha & 1 \end{bmatrix} \begin{Bmatrix} \xi'' \\ \alpha'' \end{Bmatrix} + \begin{bmatrix} \frac{2\zeta_\xi \bar{\omega}}{U^*} & 0 \\ 0 & \frac{2\zeta_\alpha \bar{\omega}}{U^*} \end{bmatrix} \begin{Bmatrix} \xi' \\ \alpha' \end{Bmatrix} + \begin{bmatrix} \left(\frac{\bar{\omega}}{U^*}\right)^2 & 0 \\ 0 & \left(\frac{1}{U^*}\right)^2 \end{bmatrix} \begin{Bmatrix} \xi \\ \alpha \end{Bmatrix} = \begin{Bmatrix} -\frac{1}{\pi\mu} C_L(\tau) \\ \frac{2}{\pi\mu r_a^2} C_m(\tau) \end{Bmatrix} \quad (2)$$

With the aerodynamic lift and moment terms C_L, C_m substituted for, a 12-state model including 4 structural and 8 aerodynamic states is obtained. Detailed expressions (including the nonlinearity) and the definition of the model parameters may be found in Edwards *et al.* [7]; only a brief description is provided here. The structural states are pitch and plunge displacements and velocities ($\alpha, \xi, \alpha', \xi'$ respectively). The aerodynamic states reproduce the role of the integro-differential terms appearing in the original model formulation, and enable representation of the overall model as a first-order linear differential equation. Any system nonlinearities (such as the plunge structural nonlinearity considered in this work) are included at this stage. All unsteady aerodynamic and gust effects are preserved and no approximations are introduced.

3.2 Interactive use of numerical model and experimental rig

The parameters of the numerical model take the form often encountered in the literature (e.g. [3, 7]). In the present numerical model, these have been tuned to reproduce dynamics that are representative of the aerofoil rig. The numerical values of the tuned parameters are provided in Table 1.

Table 1: Parameters of linear aeroelastic system

parameter	value	parameter	value	parameter	value
ω_α	28.061 (rad/s)	x_α	0.09	ζ_α	0.015
ω_ξ	16.629 (rad/s)	a_h	-0.333	b	0.175 (m)
r_α	0.40	ζ_ξ	0.015	μ	69.0

In order to achieve the first objective stated at the beginning of this section, the plots in Figure 5 showing the variation of natural frequencies and damping ratios with respect to changes in pitch and plunge stiffness were utilised.

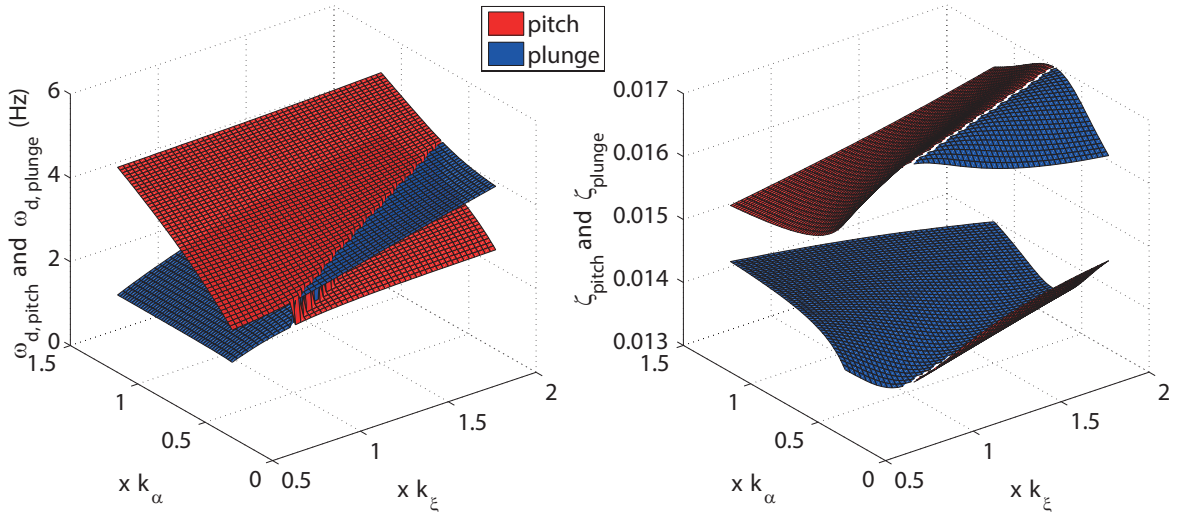


Figure 5: damped natural frequencies and damping ratios for various k_α , k_ξ

A similar plot showing the variation of flutter speed was also used. The horizontal axes in these plots show multiples with respect to the starting value of the respective stiffness in the experimental rig. Thus, one is able estimate (and subsequently implement) the required change in these parameters in order to achieve a desired combination of ω_α , ω_ξ and linear flutter speed. Since the maximum achievable airspeed in the wind tunnel is around 18 m/s, a linear flutter speed of around 14-15 m/s was desirable. Sufficient spacing between the two vibration modes was necessary, so as to ensure good quality fits to experimental FRF data especially at higher airspeeds; a minimum of separation requirement of 1 Hz was decided upon.

4 Experimental/Numerical Results Comparison

In this section, experimental observations from the aeroelastic rig are compared against predictions from numerical simulations. This is done in the frequency domain for the linear system and in the time-domain for the nonlinear system. The comparison between both sets of results will enable determination of the suitability of the numerical model in pursuing further aeroelastic experiments (e.g. active control problems).

4.1 Linear system - frequency domain

This section initially presents the experimental approach followed in acquiring the relevant data, and is followed by a discussion of the results.

4.1.1 Experimental Procedure

Two separate sets of FRF data were acquired - one resulting from control surface excitation and the other from shaker excitation of the plunge degree of freedom. The main motivation behind using shaker excitation was the inability of the control surface to apply sufficient excitation in the plunge mode, as observed from preliminary FRF data. Tests were conducted at many speeds ranging from 0 m/s up to the numerically predicted flutter speed of 15.28 m/s .

4.1.2 Data processing and comparison of results

Plots of the damped natural frequency and damping ratios against airspeed are a common means of representing aeroelastic behaviour of a linear system. Figure 6 shows these plots obtained from the numerical model, with corresponding experimental data also shown.

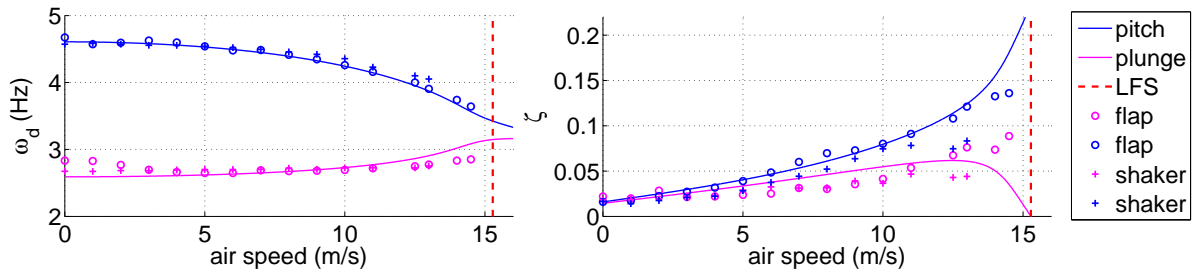


Figure 6: $V-\omega_d$ and $V-\zeta$ plots

The solid lines depict numerical results, whereas the circles and plus signs depict experimental results extracted from LMS Polymax [11] fits to frequency response data. From the first plot, it can be seen from the experimental data that there is good agreement between flap and shaker results. The only exceptions are for the plunge mode at airspeeds close to zero and for both modes close to the flutter speed (indicated by the vertical dashed line). At the lower airspeeds, the shaker results are more reliable for the reason mentioned above. Furthermore, the numerical prediction for plunge matches more closely the points generated by the shaker tests. In the pitch mode, there is excellent agreement between numerical predictions and both flap and shaker experimental results. With the damping ratios, obtaining a good quality match proved more difficult. This was exacerbated by the inability to extract meaningful data from FRF tests conducted at the vicinity of the flutter speed, an expected obstacle arising from the coalescence of the pitch and plunge modes. However, one is able to recognise clearly the similarity in the variation trends of the damping ratios between numerical and experimental results.

The final values of the parameters given in Table 1 (especially ω_α , ω_ξ , ζ_α , ζ_ξ) were arrived at after many interactive runs between experimental tests and numerical simulations. The comparison between numerical and experimental results enabled fine-tuning of the model parameters to minimise the difference between the experimental and numerically predicted dynamics.

4.2 Nonlinear system - time domain

As before, this section commences with the experimental approach, followed by a discussion of results.

4.2.1 Experimental Procedure

A standard procedure was followed to conduct the experiments; the model was placed in the wind tunnel with zero angle of attack, the nonlinearity was implemented and fixed tightly in position and the test was run for a specific freestream velocity. Once recorded the data, the nonlinearity was un-tightened and re-tightened before perform the test for a different speed. The switching on of LCO was achieved by introducing a perturbation to the steady condition of the model. The data were recorded, after all transients were decayed, for a generic 10 seconds window. The aerofoil rig begins to exhibit LCO at approximately 10.8 m/s, while the corresponding value from the numerical model is around 13.5 m/s.

4.2.2 Data processing and comparison of results

The acquired laser signal data were low-pass filtered at 30 Hz in order to remove the high frequency noise of the sensors and to emphasize the 2 *dof* dynamics respect to the flexible modes that the rig shows for frequencies higher than 40 Hz, as mentioned in Ref. [10].

The plunge nonlinearity expressed by equation eq. (1) was incorporated into the linear model, with the coefficients given in Table 4a. Results generated by the nonlinear numerical model at 15 m/s are plotted against the corresponding experimental observations in the following figures.

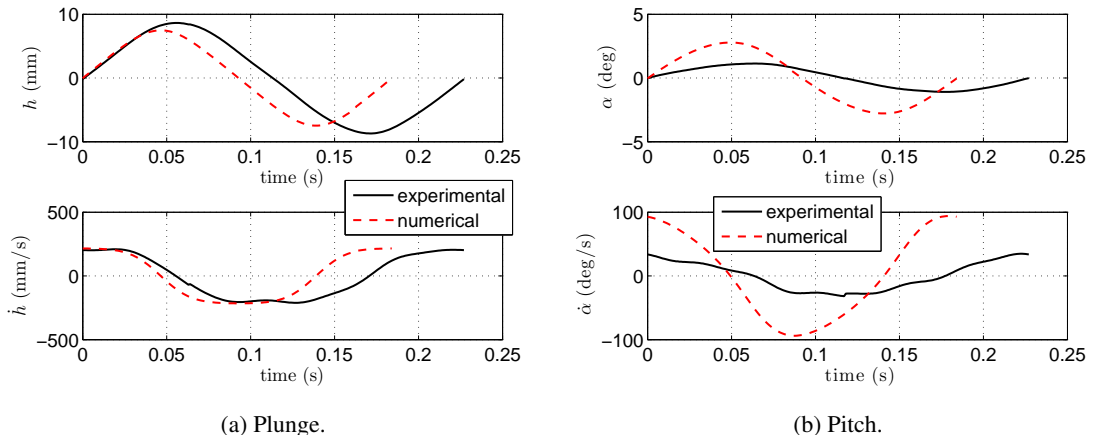


Figure 7: One period, displacement and velocity diagrams, 15 m/s.

The LCO fundamental frequency in both cases are given by the highest peaks in Figures 9. The odd harmonics expected in an LCO spectrum are also visible in both cases. In the experimental result, there also appear to be small levels of the even harmonic. Evidently, the numerical value of the fundamental LCO frequency appears to be slightly higher.

LCO response data at 15 m/s are shown in Figure 7. It is evident from plot 7a that the plunge displacements and velocities are in good agreement. Plot 7b reveals a substantial over-prediction of pitch response in the numerical model. These observations are visible more clearly from the phase-portrait diagrams in Figure 8. The trends mentioned here are similar at other airspeeds. Figure 10 shows the variation of LCO pitch and plunge amplitude and frequency for various airspeeds (normalised with respect to the linear flutter speed). Evidently, the discrepancy in displacement magnitude in plunge is much smaller than in pitch. The experimental plunge amplitude appears to remain constant, in contrast to the increase predicted numerically. In the pitch displacement, the variation trend appears to be the same in both cases. The LCO frequency values (for both pitch and plunge) are adequately close between the experimental and numerical cases. Here also, a difference in trend is evident. It was observed during the experiment that LCO ceased at approximately 10.7 m/s. Further tests will be carried out in order to understand more clearly these observations.

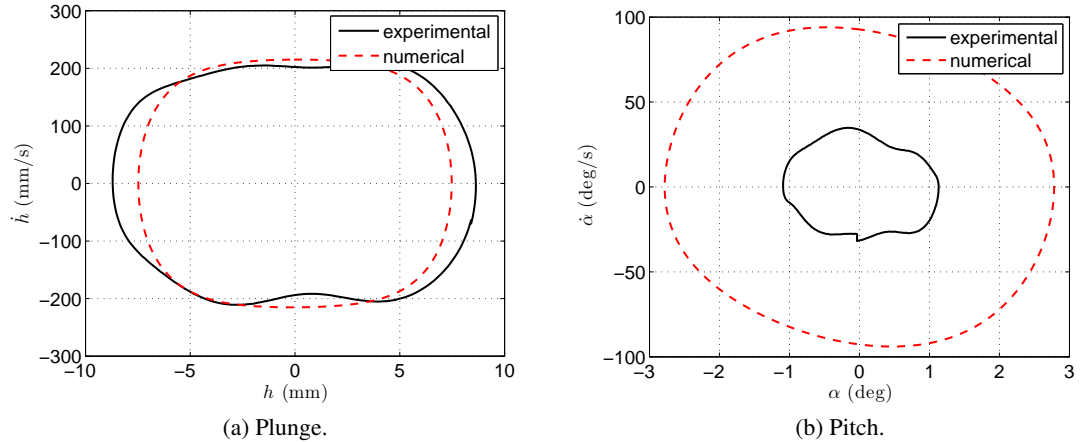


Figure 8: Phase diagrams, 15 m/s.

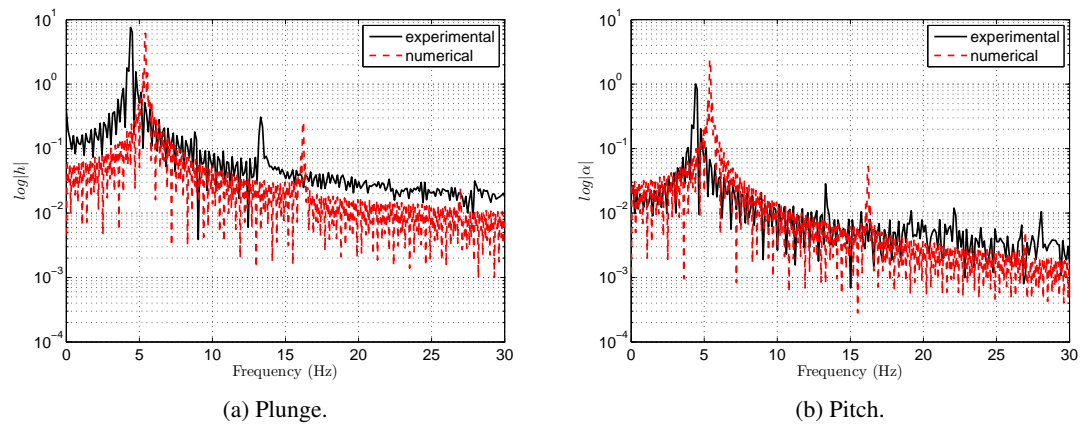


Figure 9: FFT, 15 m/s.

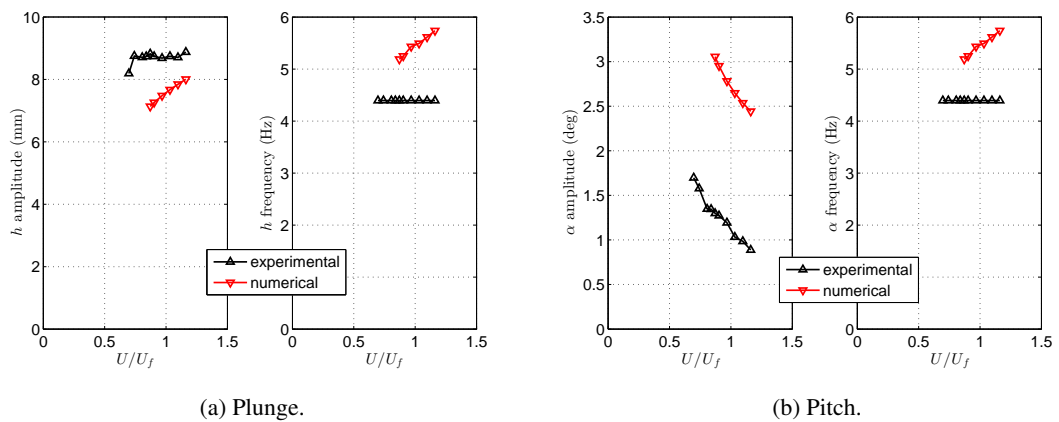


Figure 10: LCOs amplitude and frequency vs velocity.

Attempts to tune the nonlinearity coefficients and linear stiffness values without compromising the high quality tuning of the linear model (evident in Figure 6) proved inadequate in limiting the disparity between numerical and experimental pitch response. Thus, it was concluded that simultaneous tuning of the linear and nonlinear models to a high standard would initially require an investigation into the effect of all other parameters on the response, followed by the application of a methodical tuning exercise.

5 Conclusions and Remarks

The paper presented the experimental results for a 2-D, 2 *dof* nonlinear aeroelastic model, while it was undergoing LCO, for different airstream speeds, compared with numerical simulations. In the first part the experimental linear rig and its nonlinear element were described; later on, the numerical model and how it was iteratively used to achieve the best plunge/pitch values was presented. A comparison between the experimental and numerical result for the nonlinear configuration was shown as well. The overall behaviour of the two models shows a good agreement even though a more precise tuning of the nonlinear numerical model was found to be necessary; however this first comparison allowed a better understanding of the phenomena that dominates the system. This work is part of a bigger project whose final goals are to develop and test control algorithms for flutter suppression in linear and nonlinear system.

Acknowledgement

This research has been funded by EPSRC grant EP/J004987/1 under the project entitled “*Nonlinear Active Vibration Suppression in Aeroelasticity*”.

References

- [1] E. V. Ardelean. High Performance ”V-stack” Piezoelectric Actuator. *Journal of Intelligent Material Systems and Structures*, 15(11):879–889, November 2004.
- [2] Salvatore Chianetta. Limit cycle oscillations on an aerofoil test rig. Technical report, School of Engineering, University of Liverpool, U.K., 2013.
- [3] M. D. Conner, D. M. Tang, E. H. Dowell, and L. N. Virgin. Nonlinear behavior of a typical airfoil section with control surface freeplay: A numerical and experimental study. *Journal of Fluids and Structures*, 11(1):89–109, 1997. Cited By (since 1996):134.
- [4] J. Croft. Airbus elevator flutter: annoying or dangerous? *Aviation Week and Space Technology*, 155(9):41, August 2001.
- [5] Andrea Da Ronch, Nikolaos D. Tantaroudas, Kenneth J. Badcock, and John E. Mottershead. A Nonlinear Controller for Flutter Suppression: from Simulation to Wind Tunnel Testing. *55th AIAA/ASME/ASCE/AHS/SC Structures, Structural Dynamics, and Materials Conference*, pages 1–19, January 2014.
- [6] E. H. Dowell, John Edwards, and Thomas Strganac. Nonlinear aeroelasticity. *Journal of Aircraft*, 40(5):857–874, 2003.
- [7] John W. Edwards, Holt Ashley, and John V. Breakwell. Unsteady aerodynamic modeling for arbitrary motions. *AIAA J*, 17(4):365–374, 1979. Cited By (since 1996):98.
- [8] Todd O Neil, Thomas W. Strganac, and Todd O’. Aeroelastic Response of a Rigid Wing Supported by Nonlinear Springs. *Journal of Aircraft*, 35(4):616–622, July 1998.

- [9] E. Papatheou, N. D. Taroudas, A. Da Ronch, J. E. Cooper, John E. Mottershead, and A Da Ronch. Active control for flutter suppression: an experimental investigation. In *International Forum on Aeroelasticity and Structural Dynamics (IFASD)*, volume 25, page 14, Bristol, U.K., January 2013.
- [10] Evangelos Papatheou, Xiaojun Wei, Shakir Jiffri, Marco Prandina, Maryam Ghandchi Tehrani, Steven Bode, Kumar Vikram Singh, John E. Mottershead, and Jonathan Cooper. Flutter control using vibration test data: theory, rig design and preliminary results. In *International Seminar on Modal Analysis (ISMA2012)*, number Dlm, Leuven, BE, 2012.
- [11] B. Peeters, G. Lowet, H. Van der Auweraer, and J. Leuridan. A new procedure for modal parameter estimation. *Sound and Vibration*, 38(1):24–29+16, 2004. Cited By (since 1996):16.
- [12] D.S. Woolstone, H.W. Runyan, and R.E. Andrews. An investigation of effects of certain type of structural nonlinearities on wing and control surface flutter. *Journal of Aeronautical Sciences*, 24:57–63, 1957.